

PACS numbers: 42.55.Px; 42.60.Fc
DOI: 10.1070/QE2006v036n08ABEH013284

Autocorrelation function and emission spectrum of single-transverse-mode heterolasers in the self-sustained intensity pulsation regime

D.R. Miftakhutdinov, D.V. Batrak, A.P. Bogatov, A.E. Drakin, S.A. Plisyuk

Abstract. **The degree of time coherence of semiconductor lasers operating in the self-intensity pulsation regime is studied by two methods. In the first method measurements were performed with a Michelson interferometer by recording the autocorrelation function, while in the second (spectral) method the spectral density of emission was measured. It is shown that both methods give similar results; however, the spectral method can understate the degree of coherence by the value up to 30 % due to a great contribution of spontaneous emission to a recorded signal.**

Keywords: *autocorrelation function, self-sustained pulsations, semiconductor laser, end waveguide*.

1. Introduction

The degree of coherence is one of the fundamental parameters of an optical beam, in particular, a laser beam. It can be measured by using not only conventional parameters such as the emission spectrum width but also the parameters of the autocorrelation function for the optical-wave field strength. This function can be found, for example, with the help of a Michelson interferometer. The autocorrelation function of the radiation field of semiconductor lasers was studied in many papers (see, for example, [1, 2]). At present such a characterisation of time coherence in semiconductor lasers is necessary in their applications for data reading in CD devices and in various optical sensors. The matter is that a high time coherence inherent in laser beams is, as a rule, not an advantage but a disadvantage because a tight spatial focusing of the laser beam gives rise to intense noise caused by speckles.

This noise can be suppressed by different methods. One of them is the use of semiconductor lasers operating in the superluminescence regime, i.e. below the lasing threshold (see, for example, [3] and references therein). The emission spectrum of such semiconductor emitters (which are also called the edge-emitting superluminescent diodes) can be rather broad, which provides low time coherence and, hence, the averaging and smoothing of the speckle pattern, resulting in the noise suppression.

However, in this case the problem of obtaining a high enough output power appears. As a rule, the output power of a LED is lower than that of a similar device operating in the lasing regime. In this connection there exists another approach in which speckles are suppressed by using a semiconductor emitter (heterolaser) operating in the lasing regime with the additional modulation of its intensity by a high-frequency signal introduced, for example, to the pump current. Such intensity modulation is accompanied by modulation of the optical frequency (chirping) of laser modes, which can also result in the 'averaging' of speckles and, hence, in the noise suppression. This method, which was described, for example, in [4], can be most conveniently realised by using lasers capable of operating independently (without any external modulation) in a controllable self-pulsation regime. In this case, no additional high-frequency signal source is required in the feed circuit of the laser.

In any case, irrespective of the method used, the degree of 'residual' time coherence of the optical beam from a semiconductor radiation source should be controlled. Because the suppression of coherence is necessary to remove speckles, which appear due to the interference of the main beam with scattered radiation, it is obvious that the degree of coherence can be directly determined also in interferometric measurements performed, for example, by using a Michelson interferometer. However, the instruments for such interferometric measurements are less common and, as a rule, less convenient than grating monochromators and spectrometers used in spectral measurements.

It is well known that the autocorrelation function and spectral density of any quantity representing a random stationary process are related by the Fourier transform according to the Wiener – Khinchin theorem. However, in practice the validity of spectral measurements of the degree of residual time coherence and, therefore, of the noise produced by speckles is determined by the accuracy of these measurements in combination with the particular coherence of the optical beam. In this connection it is interesting to compare the results of measuring the degree of residual coherence obtained in the form of the correlation function with the help of a Michelson interferometer with the corresponding results of spectral measurements performed for heterolasers operating in the self-intensity pulsation regime.

D.R. Miftakhutdinov, D.V. Batrak, A.P. Bogatov, A.E. Drakin, S.A. Plisyuk P.N. Lebedev Physics Institute, Russian Academy of Sciences, Leninsky prosp. 53, 119991 Moscow, Russia;
e-mail: bogatov@sci.lebedev.ru

Received 20 March 2006; revision received 31 May 2006
Kvantovaya Elektronika **36** (8) 751 – 757 (2006)
Translated by M.N. Sapozhnikov

2. Experiment

We studied typical single-transverse-mode heterolasers made of quantum-well In(GaAl)P/AlGaAs/GaAs and AlGaAs/GaAs heterostructures emitting at 0.65 and 0.78 μm, respectively. The width of the active region in the horizontal direction (along the structure layers) is 3–4 μm. Waveguide properties in this direction were intentionally decreased by etching emitter p layers by the method described in [3], so that the laser waveguide was close to the gainguiding waveguide. In this case, the laser can operate in the regime of self-sustained intensity pulsations. The physical mechanism of such pulsations was considered earlier in papers [5–10], and its discussion is beyond the scope of this paper. Measurements were performed at a constant pump current at room temperature without the forced cooling of samples.

The autocorrelation function was measured with an automated Michelson interferometer, whose simplified scheme is presented in Fig. 1. Radiation from laser (*1*) passed through objective (*2*) to form a parallel light beam which was split in beamsplitter cube (*3*) into two light beams A and B. These beams reflected from mirrors (*4*) and (*5*) were focused with objective (*6*) on photodetector (*7*) (PD-26 photodiode). The output signal of the photodetector was amplified in amplifier (*8*) and recorded with computer (*9*) equipped with an analogue-to-digital converter board. Mirror (*4*) of the interferometer was mounted on movable platform (*10*) displaced with a worm gear. Worm shaft (*11*) was rotated with step motor (*12*) controlled with a computer via control unit (*13*). The step motor had a step of one thousandth of a full turn, while a pitch of the worm was 1 mm, which provided the positioning of mirror (*4*) on average with a step of 1 μm. Mirror (*5*) was mounted on piezoceramic cylinder (*14*) to which a sinusoidal voltage was applied from a generator, which was recorded with the computer. The voltage amplitude applied across the piezoceramic cylinder excited oscillations of mirror (*5*) with the controllable amplitude $\sim 1-2$ μm.

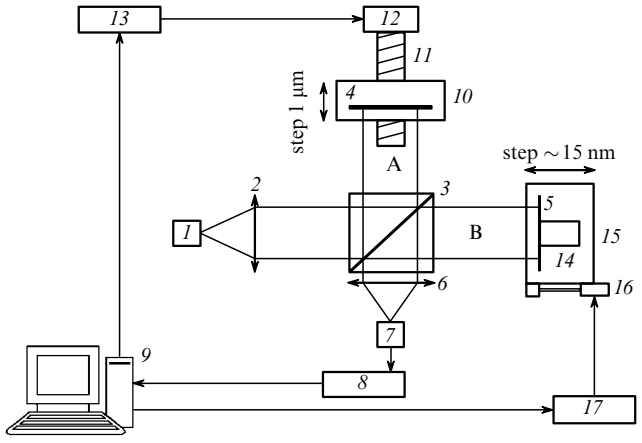

Figure 1. Scheme of the interferometer: (*1*) radiation source (laser or LED); (*2*, *6*) objectives; (*3*) beamsplitter cube; (*4*, *5*) mirrors; (*7*) photodiode; (*8*) amplifier; (*9*) computer; (*10*, *15*) translation platforms; (*11*) worm shaft; (*12*) step motor; (*13*) step-motor control unit; (*14*) piezoceramic cylinder; (*16*) piezoceramic translator; (*17*) piezoceramic-translator control unit.

The piezoelectric with a mirror was mounted on stage (*15*) which could be moved with an irregular but controllable step with the help of piezoelectric step translator (*16*) controlled with the computer via control unit (*17*). The use of periodic sinusoidal oscillations of the mirror in combination with a small (compared to the oscillation amplitude) step movement allowed us to calibrate this step movement, thereby varying the path difference in the interferometer by moving mirror (*5*) with a step of ~ 50 mm [the path difference could be varied from -5 to 70 cm by moving mirror (*4*)].

The results of measurements were processed as follows. Let us represent the strengths of quasi-monochromatic fields produced by beams A and B on the photosensitive surface of a photodetector in the form

$$\mathscr{E}_{\mathrm{A}}(t) = \mathscr{E}(t) = E(t)\exp(-\mathrm{i}\omega t) + \mathrm{c.c.},$$

$$\mathscr{E}_{\mathrm{B}}(t) = \alpha\mathscr{E}(t+\tau)$$

$$= \alpha E(t+\tau)\exp[-\mathrm{i}\omega(t+\tau)] + \mathrm{c.c.}, \qquad (1)$$

where $E(t)$ is the slowly varying complex amplitude; ω is the central frequency; τ is the path difference for beams A and B; α is a positive coefficient close to unity, which characterises the intensity unbalance between beams A and B, which is always present due to the imperfection of optical systems (in our case, this unbalance was 0.8–0.9). We assume for simplicity that the field amplitude is measured in units in which the intensity coincides with the time-averaged square of the field amplitude. In this case, the intensity I on the photodetector can be written as

$$I = I_0[1 + \eta\psi(\tau)],$$

$$I_0 = (1+\alpha^2)\overline{\mathscr{E}^2(t)}, \quad \eta = \frac{2\alpha}{1+\alpha^2}, \qquad (2)$$

$$\psi(\tau) = \overline{\mathscr{E}(t)\mathscr{E}(t+\tau)} \Big/ \overline{\mathscr{E}^2(t)},$$

where I_0 the total intensity of beams A and B; $\psi(\tau)$ is the normalised autocorrelation function for the field $\mathscr{E}(t)$; and η is a positive coefficient close to unity ($\eta \leqslant 1$).

By using relations (1), we can represent the autocorrelation function in the form

$$\psi(\tau) = v(\tau)\cos[\omega\tau + \varphi(\tau)],$$

$$v(\tau) = |\overline{E(t)E^*(t+\tau)}| \Big/ |\overline{E^2(t)}|, \qquad (3)$$

$$\exp[\mathrm{i}\varphi(\tau)] = \overline{E(t)E^*(t+\tau)} \Big/ |\overline{E(t)E^*(t+\tau)}|.$$

The presence of cosine in expression (3) for the autocorrelation function corresponds to the well-known interference pattern in which the intensity I oscillates from the maximum $I_{\max}$ to minimum value $I_{\min}$ when the cosine argument

$$\Phi(\tau) = \omega\tau + \varphi(\tau) \qquad (4)$$

varies due to a change in the path difference τ. The envelope of these oscillations $v(\tau)$ coincides with an

accuracy to the factor η with the visibility $u(\tau)$ of the interference pattern:

$$u(\tau) = \frac{I_{\max} - I_{\min}}{I_{\max} + I} = \eta v(\tau). \quad (5)$$

The experimental data obtained with a Michelson interferometer were processed to obtain the dependences of the visibility of the interference pattern $u(\tau)$ and the cosine argument on the path difference $\Phi(\tau)$. By using expressions (3)–(5) and the Wiener–Khinchin theorem, we found the spectral density for the field amplitude $\mathscr{E}(t)$. The data were processed assuming that η is independent of τ.

The spectral density, the spatial distribution of the radiation intensity, and pulsation frequencies of the output power of the laser were measured by standard methods described in [11, 12]. A DFS-24 spectrometer with a spectral resolution of 0.03 nm (according to the Rayleigh criterion) was used. The envelope of the autocorrelation function was calculated by using the Fourier transform.

Figure 2 presents typical emission characteristics of lasers emitting at 0.65 μm. It follows from the light–current characteristic (Fig. 2a) that the lasing threshold is ~53 mA. This is the expected value for lasers in which waveguide properties of the active region in the horizontal direction are mainly formed due to amplification. The same concerns the slope efficiency. In this respect, lasers of this type are inferior to lasers with a waveguide formed only by the refractive index profile. However, their main advantage is that they exhibit distinct self-sustained intensity pulsations already slightly above the lasing threshold. As mentioned above, pulsations cause mode chirping and, hence, the broadening of spectral lines corresponding to each longitudinal mode. One can see this by comparing the spectrum at the threshold (Fig. 2b), when chirping is negligible, with the spectra in Figs 2c and d in which chirping is present.

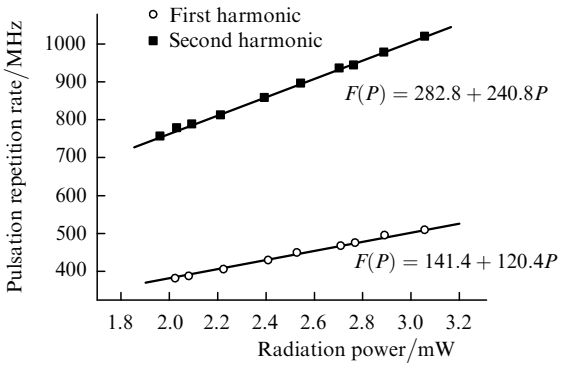

Figure 3. Dependences of the pulsation repetition rate F for the first and second harmonics on the radiation power P for a 0.65-μm laser.

The repetition rate of such pulsations linearly depends on the average laser power or pump current. This circumstance was pointed out earlier in [13] and is demonstrated in Fig. 3. The results were obtained by detecting the output signal of a fast photodetector with a selective DNIS-4 voltmeter. In this case, the amplitudes of the first and second harmonics were close, which suggests that intensity pulsations considerably differ from harmonic pulsations and have a large depth.

An important property of lasers operating in the self-sustained pulsation regime is the dynamic dependence of the optical beam width on the laser power. This concerns both the instantaneous (described in detail in [9]) and average values. Thus, Fig. 4 presents the far-field radiation distributions and the width of the radiation pattern demonstrating the decrease in the divergence (the increase in the effective beam width in the active region) with increasing pump current.

Figure 5 presents the visibility of interference $u(\tau)$ (5) measured for two pump currents. On the abscissa the path difference $\Delta l = c\tau$, where c is the speed of light, is also

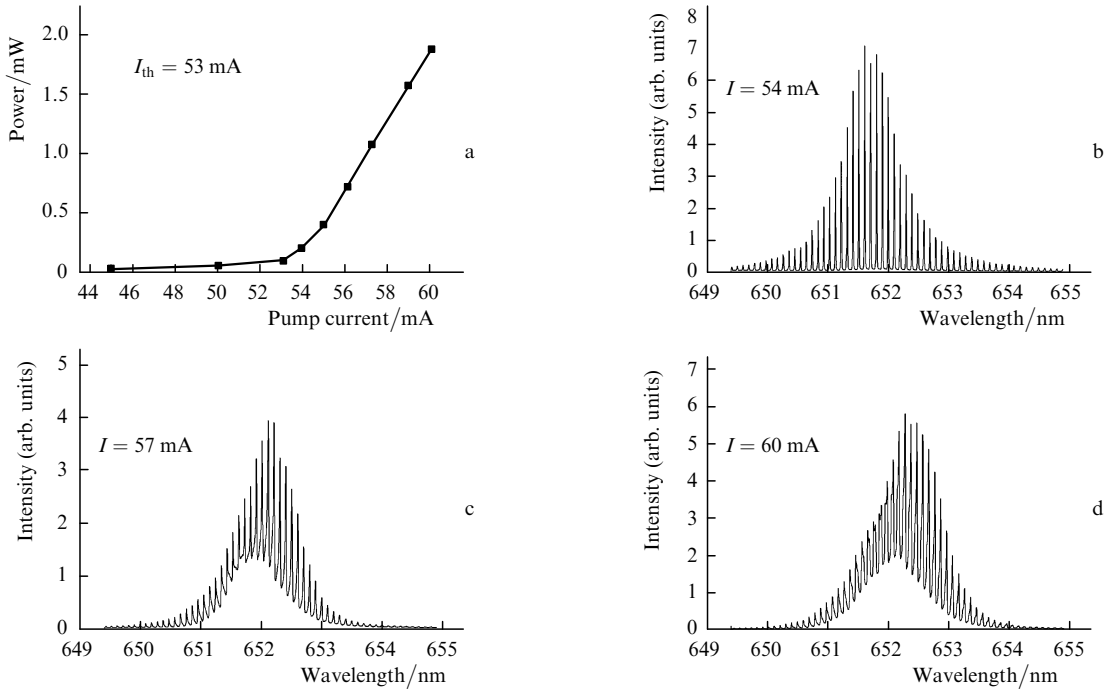

Figure 2. Emission characteristics of a 0.65-μm laser: (a) light–current characteristic and (b–d) emission spectra for different pump currents.

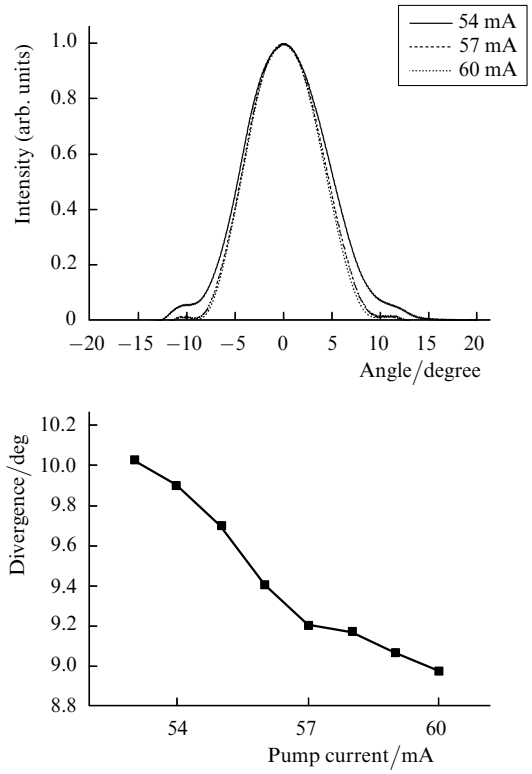

Figure 4. Dependences of the divergence in the p–n junction plane on the pump current for a 0.65-μm laser (at the top is presented the radiation pattern, at the bottom – the half-width of the radiation pattern).

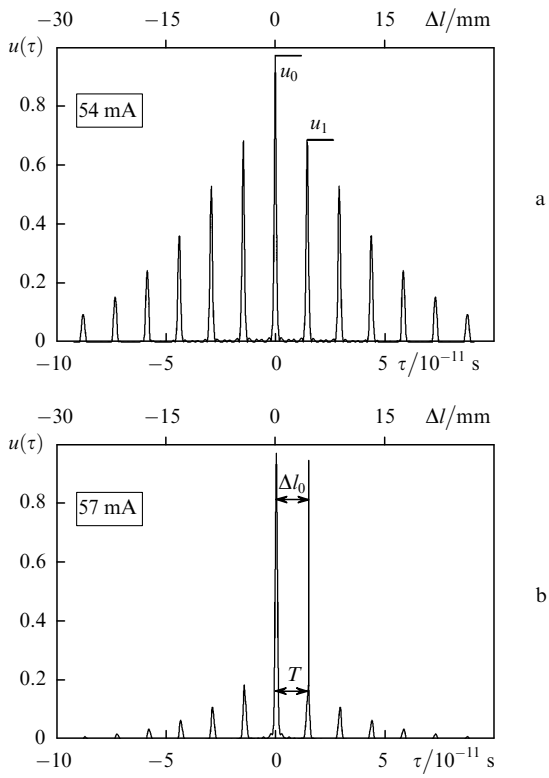

Figure 5. Visibility of the interference pattern for pump currents 54 (a) and 57 mA (b).

plotted along with time. The repetition period T of characteristic peaks is determined by the cavity round-trip transit time of a wave packet formed by several longitudinal modes:

$$T = \frac{2Ln^*}{c} = \frac{\Delta l_0}{c}, \tag{6}$$

where Δl_0 the distance between the peaks; n^* is the effective group refractive index; and L is the laser diode length. This period is related to the longitudinal mode distance over frequency $\Delta\omega$ or wavelength $\delta\lambda$ by the expressions

$$\Delta\omega = \frac{2\pi}{T} = \frac{\pi c}{Ln^*}, \quad \delta\lambda = \frac{\Delta\omega}{\omega}\lambda = \frac{\lambda^2}{2Ln^*}. \tag{7}$$

The expected behaviour of the dependence $u(\tau)$ is a decrease in the peak amplitude with increasing τ, which is determined by the width of an individual longitudinal mode, in our case – by its broadening due to chirping. Therefore, the decrease in the peak amplitude with increasing τ characterises the degree of time coherence. In a number of practical cases, the quantitative criterion

$$\gamma = \frac{u_1}{u_0} \tag{8}$$

is used to describe this behaviour, where u_1 is the first peak amplitude and u_0 is the zero peak amplitude (Fig. 5a). The value of γ is the best quantitative characteristic of the intensity of speckles and, hence, of the speckle noise The admissible value of γ depends on a particular application. For example, for CD systems it is often required that γ would not exceed 0.7, while in coherent optical tomography the requirement are considerably higher, and values $\gamma \lesssim 10^{-2}$ are considered acceptable. A comparison of Figs 5a and b shows that γ decreases with increasing current. This is also demonstrated indirectly by Fig. 2 where the chirping effect increases with increasing the pump current.

According to the above discussion, the visibility $u(\tau)$ can be also calculated from the spectra similar to those shown in Fig. 2 by using the Wiener–Khinchin relation. The result of such calculation in Fig. 6 is compared with direct measurements performed with a Michelson interferometer.

The results of spectral and interferometric measurements coincide qualitatively. However, the value of γ obtained from spectral measurements is lower than that value obtained directly from interferometric measurements.

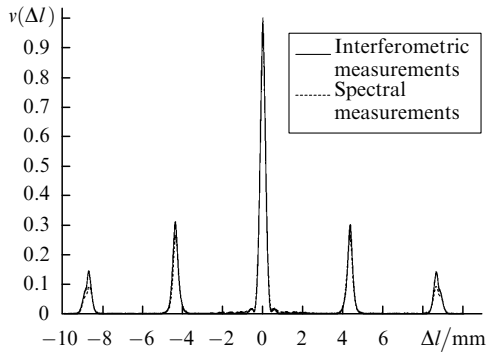

Figure 6. Envelopes of the autocorrelation function obtained in interferometric and spectral measurements.

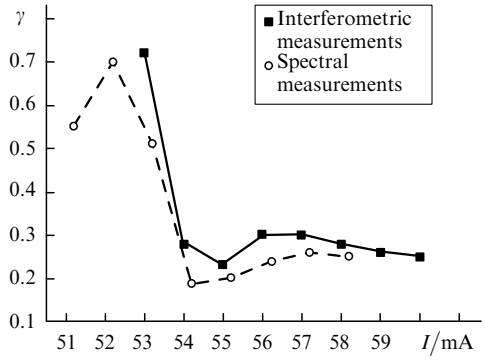

Figure 7. Values of γ factors for a 0.65-μm laser obtained from interferometric and spectral measurements.

This is shown in more detail in Fig. 7 demonstrating the dependence of the parameter γ on the pump current of the laser whose spectra are presented in Fig. 2. Nevertheless, the general behaviour of γ on the pump current obtained by both methods coincides quite well. The maximum value of $\gamma \simeq 0.8$ is observed near the lasing threshold. The self-pulsation threshold in these samples virtually coincides with the lasing threshold. As a result, γ begins to fall at once after the beginning of lasing and then is stabilised at a level of ~ 0.3. In this case, the discrepancy in the values of γ found by different methods is less than 0.1, which gives the relative error not exceeding $\sim 30\,\%$.

Similar measurements were performed for lasers emitting at 0.78 μm. Figure 8 presents typical emission parameters of these lasers. As a whole, their behaviour is similar to that of lasers emitting at 0.65 μm. The quantitative difference is observed between threshold currents, which is most likely explained by a higher differential amplification in AlGaAs/GaAs lasers compared to that in $In_{0.49}(GaAl)_{0.51}P$/AlGaAs/GaAs lasers. In addition, there exists the qualitative difference consisting in the presence of the intense amplified spontaneous emission with the TM polarisation near the lasing threshold. This is most distinctly demonstrated in Fig. 8b where along with sharp peaks corresponding to the TE modes the broader peaks corresponding to the TM

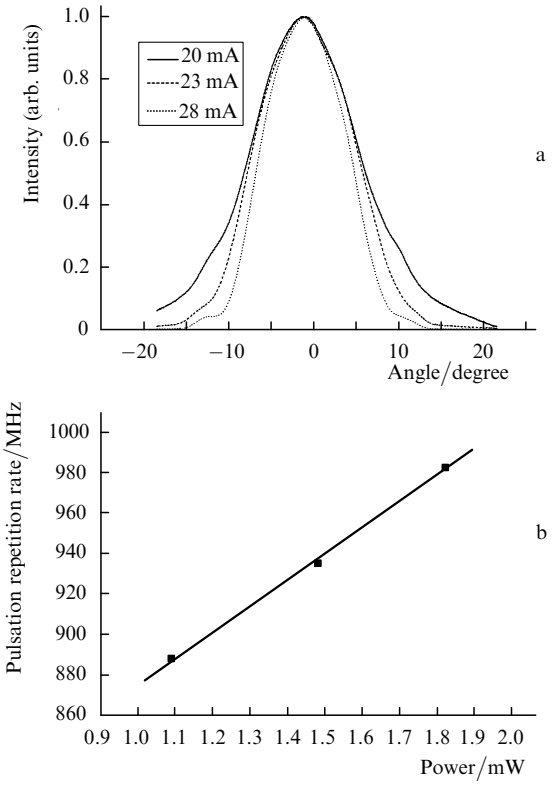

Figure 9. Dependences of the radiation pattern in the p–n junction plane on the pump current (a) and of the pulsation repetition rate on the radiation power (b) for a 0.78-μm laser.

modes are present. The envelope of these broad peaks is shifted to the blue with respect to the TE modes at which lasing occurs. The characteristic change in the time-averaged radiation pattern caused by self-pulsations in these lasers is shown in Fig. 9. This figure also shows the dependence of the pulsation repetition rate on the laser output power. Note that compared to lasers emitting at 0.65 μm, the range of pulse repetition rate is shifted to the blue. This also qualitatively agrees with a higher differential amplification in AlGaAs/GaAs lasers.

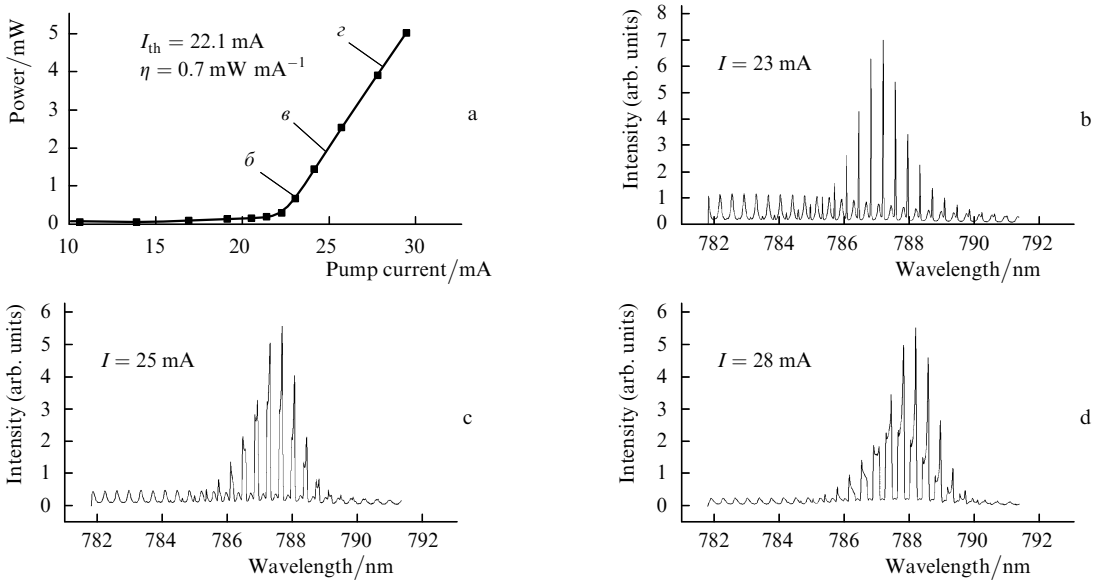

Figure 8. Emission characteristics of a 0.78-μm laser: (a) light–current characteristic and (b–d) emission spectra for different pump currents.

Figure 10 demonstrate the dependence of the coherence parameter γ on the pump current for lasers of this type. The solid curve presents the results of interferometric measurements and the lower dotted curve corresponds to spectral measurements. Note that the discrepancy of results obtained by different methods for lasers of this type is greater than that for In(GaAl)GaAs lasers. This discrepancy is most likely explained by an intense amplified spontaneous emission in the emission spectra of AlGaAs/GaAs lasers. Indeed, the filtration of the TM polarisation component in the emission spectrum (dashed curve in Fig. 10) considerably improves the agreement between the values of γ obtained by different methods. The TM component was filtered by the manual processing of the recorded spectrum because filtration by using a polariser considerably changed the laser dynamics.

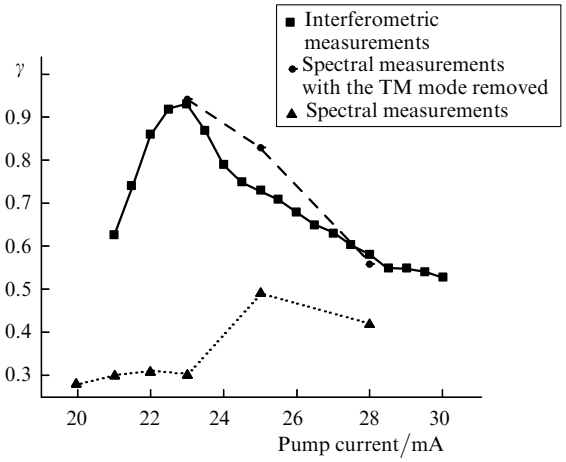

Figure 10. Values of γ factors for a 0.78-μm laser obtained from interferometric and spectral measurements with and without filtration of the TM mode in the emission spectrum.

It was interesting to verify the above-considered methods in the inverse problem of reconstructing the spectral density of radiation from interferometric measurements. We used for this purpose an edge-emitting superluminescent AlGaAs/GaAs LED with a mesastrip tilted to the facets. The corresponding autocorrelation function is presented in Fig. 11a. Figure 11b shows the spectra calculated from the autocorrelation function by using the Wiener–Khinchin relations and measured directly with an MDR-4 monochromator equipped with a PD-24 photodiode. Although the half-widths of the curves in Fig. 11b are close, the long-wavelength wings of the spectra are different. The long-wavelength wing obtained in direct measurements is less intense than that calculated from the autocorrelation function. This can be explained by different spectral sensitivities by photodetectors used in experiments and a lower efficiency of the diffraction grating of the monochromator in the long-wavelength region.

3. Discussion of results and conclusions

An analysis of the data characterising the degree of time coherence of semiconductor lasers operating in the self-pulsation regime has shown that the results of spectral measurements are adequate to interferometric measurements. The parameter γ can be understated in spectral

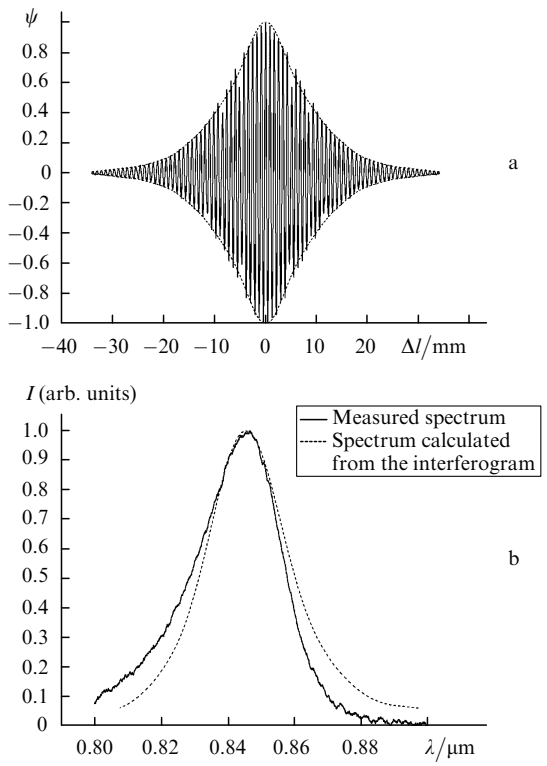

Figure 11. Autocorrelation function (a) and emission spectra (b) calculated from the autocorrelation function (dashed curve) and recorded with a spectrometer (solid curve) for an end LED.

measurements no more than by 30% for the following two reasons. The first one is the insufficient measurement accuracy. Spectral measurements give the data on the spectral density of radiation in the form of the convolution of the spectral density with the instrumental function of a spectrometer. Therefore, the relation between the spectral width of the instrumental function and the 'true' broadening of a mode caused by pulsations is important. In any case, the instrumental function broadens the spectral width of the mode recorded in experiments, thereby understating the value of γ. This was observed to a greater or lesser extent in experiments. The measurement error of γ is determined by the relation between the real spectral width of the mode, the width of the instrumental function of a spectral instrument, and the mode interval. Indeed, γ characterises by definition the ratio between the mode width $\delta\omega$ and mode interval $\Delta\omega$. If the ratio $\delta\omega/\Delta\omega \to 0$, then $\gamma \to 1$, and vice versa, $\delta\omega/\Delta\omega \to 1$, we have $\gamma \to 0$. Therefore, to measure γ correctly for the characterisation of lasers by the residual coherence parameter, the width $\delta\omega_{ap}$ of the instrumental function of the spectral instrument should be smaller than the mode interval $\Delta\omega$.

Another possible reason for understating the value of γ is the influence of amplified spontaneous emission. Because the aperture ratio of a spectrometer is higher than that of a Michelson interferometer, the measured spectral density contains a large contribution of spontaneous emission, which additionally broadens the mode spectrum. Spontaneous emission in a Michelson interferometer has no effect on the interference pattern because of its spatial coherence. It is also obvious that the requirements to spectral measurements of the degree of coherence of edge-emitting superluminescent diodes are much higher than to such

measurements for lasers. In this case, apart from a high spectral resolution of the instrument, a high degree of the spatial filtration of the optical beam should be provided.

Our study has confirmed the interrelation between the formation of the emission spectrum in semiconductor lasers and the dynamics of its intensity. The self-pulsation regime appeared in the studied lasers at the lasing threshold. This nonstationary behaviour resulted in the generation of many longitudinal modes and the spectral broadening of individual modes. Self-pulsations caused by the deformation (change in the width) of the transverse intensity distribution in a 'weak' waveguide provide a deep intensity modulation, which is demonstrated by strong chirping. The pulsation frequency almost linearly depends on the average power or (which is almost the same) the pump current.

Acknowledgements. This work was partially supported by the Presidium of RAS program 'Low-dimensional quantum structures' and the DPS of RAS program 'Coherent optical radiation of semiconductor compounds and structures'.

References

1. Vvedenskii B.S., Logginov A.S., Senatorov K.Ya. *Kvantovaya Elektron.*, 1, 1232 (1974) [*Sov. J. Quantum Electron.*, 4, 678 (1974)].
2. Bachert H., Eliseev P.G., Manko M.A., Strahov V.P., Raab S., Thay C.M. *IEEE J. Quantum Electron.*, **11** (7), 507 (1975).
3. Mamedov D.S., Prokhorov V.V., Yakubovich S.D. *Kvantovaya Elektron.*, **33**, 471 (2003) [*Quantum Electron.*, 33, 471 (2003)].
4. Nemoto K., Kamei T., Abe H., Imanishi D., Narui H., Hirata S. *Appl. Phys. Lett.*, **78** (16), 2270 (2001).
5. Bahert H.-U., Bogatov A.P., Eliseev P.G. *Kvantovaya Elektron.*, **5**, 603 (1978) [*Sov. J. Quantum Electron.*, **8**, 346 (1978)].
6. Bogatov A.P., Gurov Yu.V., Eliseev P.G., Okhotnikov O.G., Pak G.T., Khairetdinov K.A. *Sol.-State Electron Devices*, **3** (3), 72 (1979).
7. Roy Lang. *Jap. J. Appl. Phys.*, **19** (2), L93 (1980).
8. Van der Ziel J.P. *IEEE J. Quantum Electron.*, **17** (1), 60 (1981).
9. Chang-Zhi Guo, Kai-Ge Wang. *IEEE Trans. Microwave Theory Techn.*, **MTT-30** (10), 1716 (1982).
10. Bogatov A.P., Duraev V.P., Eliseev P.G., Luk'yanov S.A. *Kvantovaya Elektron.*, **15**, 1552 (1988) [*Sov. J. Quantum Electron.*, **18**, 971 (1988)].
11. Bogatov A.P., Boltaseva A.E., Drakin A.E., Belkin M.A., Konyaev V.P. *Kvantovaya Elektron.*, **30**, 315 (2000) [*Quantum Electron.*, **30**, 315 (2000)].
12. Bogatov A.P., Drakin A.E., Stratonnikov A.A., Konyaev V.P. *Kvantovaya Elektron.*, **30**, 401 (2000) [*Quantum Electron.*, **30**, 401 (2000)].
13. Bogatov A.P., Eliseev P.G., Kobildzhanov O.A., Madgazin V.P., Khaidarov A.V. *Kratk. Soobshch. Fiz. FIAN*, No. 1, 16 (1987).